

# Lawrence Berkeley National Laboratory

## Recent Work

### Title

BEHAVIOR OF POWER LIMITED TRANSVERSE STOCHASTIC COOLING SYSTEMS

### Permalink

<https://escholarship.org/uc/item/9d96d5dk>

### Author

Goldberg, G.R. Lambertson D.A.

### Publication Date

1988-07-01

c.2



# Lawrence Berkeley Laboratory

UNIVERSITY OF CALIFORNIA

## Accelerator & Fusion Research Division

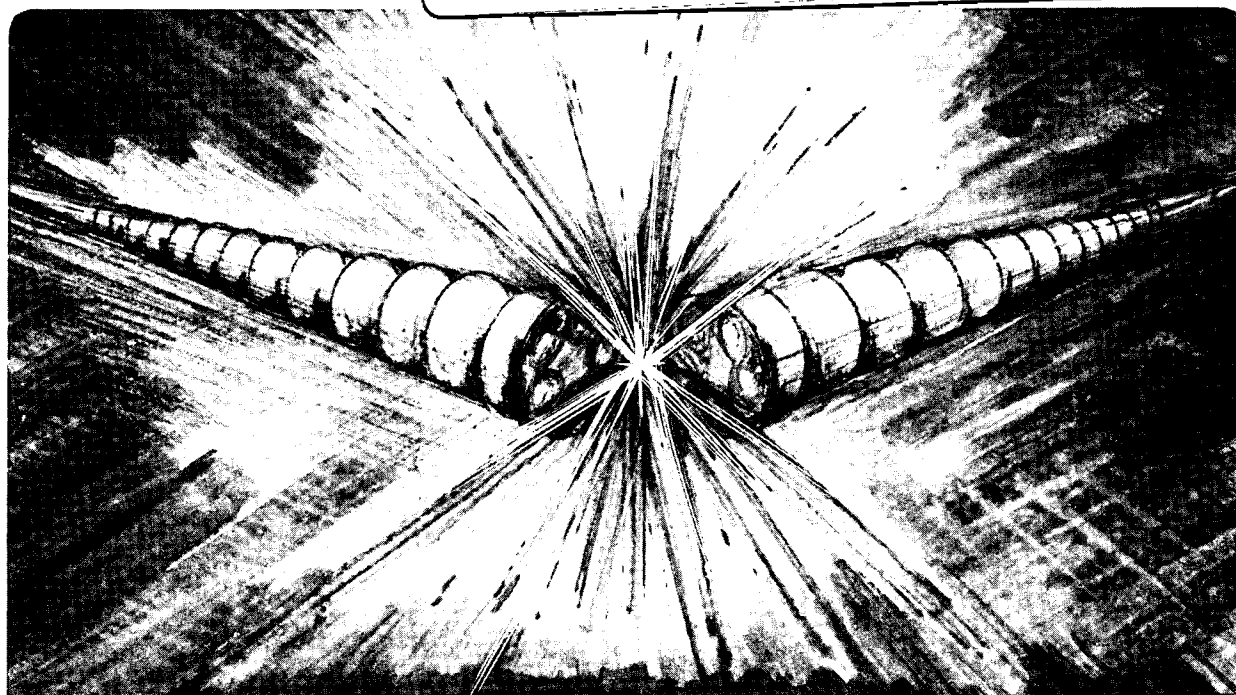
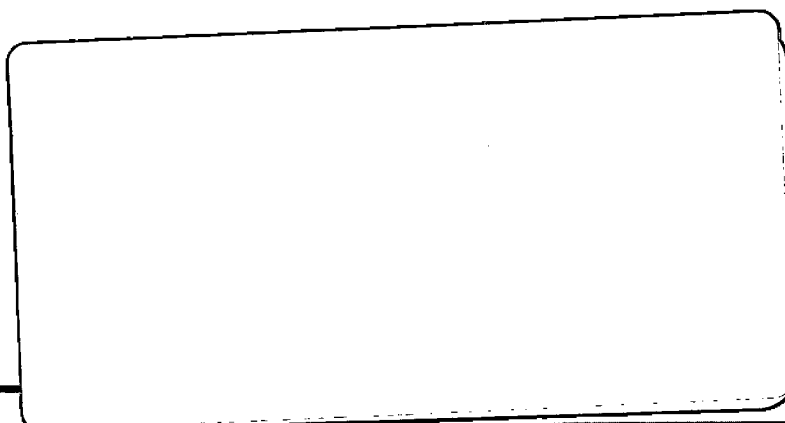
**Behavior of Power-Limited Transverse Stochastic  
Cooling Systems**

SEP 15 1983

D.A. Goldberg and G.R. Lambertson

RECEIVED  
DOCUMENTS SECTION

July 1988



LBL-24979  
c.2

## **DISCLAIMER**

This document was prepared as an account of work sponsored by the United States Government. While this document is believed to contain correct information, neither the United States Government nor any agency thereof, nor the Regents of the University of California, nor any of their employees, makes any warranty, express or implied, or assumes any legal responsibility for the accuracy, completeness, or usefulness of any information, apparatus, product, or process disclosed, or represents that its use would not infringe privately owned rights. Reference herein to any specific commercial product, process, or service by its trade name, trademark, manufacturer, or otherwise, does not necessarily constitute or imply its endorsement, recommendation, or favoring by the United States Government or any agency thereof, or the Regents of the University of California. The views and opinions of authors expressed herein do not necessarily state or reflect those of the United States Government or any agency thereof or the Regents of the University of California.

**BEHAVIOR OF POWER-LIMITED TRANSVERSE STOCHASTIC  
COOLING SYSTEMS\***

D.A. Goldberg and G.R. Lambertson  
Lawrence Berkeley Laboratory  
University of California  
Berkeley, CA 94720

July 1988

\*This work was supported by the Director, Office of Energy Research, Office of High Energy and Nuclear Physics, High Energy Physics Division, U.S. Dept. of Energy, under Contract No. DE-AC03-76SF00098.

BEHAVIOR OF POWER-LIMITED TRANSVERSE STOCHASTIC COOLING SYSTEMS \*

D.A. Goldberg and G.R. Lambertson  
 Lawrence Berkeley Laboratory

Introduction

Analysis of stochastic cooling systems is usually done under the assumption that the system performance is not limited by the available electronic gain. In practical systems, it may prove to be the case that cost-induced limitations on the maximum available output power restrict the maximum attainable gain, thereby restricting it to be less than its optimal value. Such is the case in the anti-proton sources at both CERN and Fermilab. The criteria that one would employ in, for example, upgrading such a power-limited system prove to be rather different from those for a system for which one can optimize the gain.

In the following sections we first develop the formulas relevant to the behavior of power-limited cooling systems; we limit our treatment throughout to the case of systems which cool the transverse phase space of the beam. We then discuss the implications of our results for the upgrade of such cooling systems, contrasting this case with that for systems in which the electronic gain can be optimized. Finally, we apply our results to the specific case of the Fermilab debuncher ring.

Formulary for Power-Limited Systems

The usual expression for the cooling rate of a stochastic cooling system is [1]

$$\frac{1}{\tau} = \frac{W}{N} [2g - g^2(M+U)] \quad (1)$$

where  $g$ , is usually referred to as the system gain; in a transverse cooling system, it represents the fraction of the beam-sample centroid error corrected in a single pass through the pickup and kicker. The usual procedure is to minimize  $\tau$  by setting  $g = 1/(M+U)$ , its optimum value, thereby yielding the familiar result

$$\frac{1}{\tau_{opt}} = \frac{W}{N(M+U)} \quad (2)$$

One can formally express the system gain as

$$g = \mathcal{G} \cdot G \quad (3)$$

where  $G$  represents the electronic (voltage) amplification, and  $\mathcal{G}$  includes everything else (i.e. pickups, kickers, external circuit losses, etc.). Expressing  $\mathcal{G}$  in terms of the various system parameters, we have

$$\mathcal{G} = \frac{\alpha \bar{\beta} n_L K_L Z'_L N e f_o}{\sqrt{2} E/e} = \frac{e f_o c \bar{\beta} \alpha N}{\sqrt{2} \pi E/e f_B} \frac{n_L Z'_L{}^2}{Z_c} \quad (4)$$

where

$N$  = total number of particles

$\alpha$  = voltage attenuation in the pickup and kicker circuitry located between the electrodes and the amplifier circuits

$\bar{\beta}$  = (geometric) mean of the beta functions at the pickup and kicker

$e$  = proton charge

\* Work supported by the Director, Office of Energy Research, Office of High Energy and Nuclear Physics, High Energy Physics Division, U.S. D.O.E., under Contract No. DE-AC03-76SF00098.

$f_o$  = particle revolution frequency

$c$  = velocity of light

$n_L$  = number of kicker/pickup loop pairs

$Z_L'$  = single-loop-pair (transverse) transfer impedance

$K_L$  = single-loop-pair (transverse) kicker constant =  $cZ_L'/\pi f_B Z_C$

$f_B$  = mid-band beam (signal) frequency

$Z_C$  = characteristic impedance of external signal lines

$E$  = total proton energy (rest + kinetic)

Let us now define  $G_{lim}$  as the maximum available (i.e. power-limited) electronic gain, and  $G_{opt}$  as the gain required to yield  $g_{opt} = 1/(M+U)$ . We can then write

$$g_{lim} = \mathcal{G} \cdot G_{lim} \quad (5a)$$

and

$$g_{opt} = \mathcal{G} \cdot G_{opt} \quad (5b)$$

From Eq. 1, we have for the power-limited  $\tau_{lim}$

$$\frac{1}{\tau_{lim}} = \frac{W}{N} [2g_{lim} - 2g_{lim}^2 (M+U)] = \frac{W}{N} g_{lim} [2 - \frac{g_{lim}}{g_{opt}}]$$

Making use of Eqs. 5a and 5b gives

$$\frac{1}{\tau_{lim}} = \frac{1}{\tau_{opt}} \frac{G_{lim}}{G_{opt}} [2 - \frac{G_{lim}}{G_{opt}}] \quad (6a)$$

or

$$\frac{1}{\tau_{lim}} = \frac{1}{\tau_p} [2 - \frac{G_{lim}}{G_{opt}}] \quad (6b)$$

where, for analyzing power-limited systems, it is convenient to introduce the quantity

$$\frac{1}{\tau_p} \equiv \frac{1}{\tau_{opt}} \frac{G_{lim}}{G_{opt}} \quad (7a)$$

We now seek to obtain expressions for  $G_{lim} / G_{opt}$  and  $\tau_p$ . From Eq. 5b we have

$$G_{opt} = [\mathcal{G} (M+U)]^{-1} \quad (8)$$

Substituting Eqs. 2 and 8 in Eq. 7a gives

$$\frac{1}{\tau_p} = \frac{W \mathcal{G} G_{lim}}{N} \quad (7b)$$

The quantity  $G_{lim}$  is simply the square root of  $P_{out} / P_{in}$ , where  $P_{out}$  is the maximum available output power, and  $P_{in}$  is the sum of the noise and signal power at the input, which can also be expressed as  $(1 + U^{-1})$  times the input noise power. Expressing the latter in terms of  $T_R$  and  $T_A$ ,

the equivalent noise temperatures of the input circuit and preamplifier, respectively we have

$$G_{lim} = \sqrt{\frac{P_{out}}{(1 + \frac{1}{U}) k (T_R + T_A) W}} \quad (9)$$

where  $W$  is the electronic bandwidth. Substituting Eqs. 4 and 9 in 7b, we obtain

$$\frac{1}{\tau_p} = \frac{e c f_o \bar{\beta} \alpha n_L (Z'_L)^2}{\sqrt{2} \pi E/e f_B Z_c} \sqrt{\frac{P_{out} W}{(1 + \frac{1}{U}) k (T_R + T_A)}} \quad (10)$$

If one has already calculated  $\tau_{opt}$  one can now use Eq. 7a to obtain

$$\frac{G_{lim}}{G_{opt}} = \frac{\tau_{opt}}{\tau_p} \quad (11a)$$

To calculate the ratio directly, we combine Eqs. 4, 8, and 9 to obtain

$$\frac{G_{lim}}{G_{opt}} = \frac{e c f_o \bar{\beta} \alpha n_L (Z'_L)^2 N (M+U)}{\sqrt{2} \pi E/e f_B Z_c} \sqrt{\frac{P_{out}}{(1 + \frac{1}{U}) k (T_R + T_A) W}} \quad (11b)$$

To evaluate either Eq. 2 or 9, we use for the noise-to-signal ratio  $U$  the expression

$$U = \frac{2 \pi k (T_R + T_A)}{N e^2 f_o \beta_x \bar{\epsilon} \alpha_p^2} \frac{Z_c}{n_L Z'_L{}^2} \quad (12)$$

where  $\alpha_p$  is the voltage attenuation factor for the external pickup electronics, and the average emittance  $\bar{\epsilon}$  is defined by the relation

$$\langle x^2 \rangle = \beta_x \bar{\epsilon} / 2\pi \quad (13)$$

where  $\beta_x$  is the beta function at the pickup, and for a (2-dimensional) Gaussian emittance distribution,  $\bar{\epsilon} \approx \epsilon_{95}/3$ . Note that in the limit that  $U \gg M$ ,  $N (M+U) \approx NU$ , and so in this limit

$$\frac{G_{lim}}{G_{opt}} = \frac{c}{\sqrt{2} E/e f_B \bar{\epsilon}} \frac{\bar{\beta} \alpha}{\beta_x \alpha_p^2} \sqrt{\frac{P_{out} (T_R + T_A)}{W}} \quad (14)$$

Finally, to evaluate the ability of a system to cool a beam from an initial emittance  $\epsilon_i$  to a final emittance  $\epsilon_f$ , one can make use of the relation

$$\frac{d\epsilon}{\epsilon} = -\frac{dt}{\tau} \quad (15)$$

to calculate the total cooling time  $T_{tot}$ .

$$T_{tot} = - \int_{\epsilon_i}^{\epsilon_f} \frac{\tau(\epsilon) d\epsilon}{\epsilon} \quad (16)$$

## General Conclusions

Several striking conclusions can be drawn from the above results. Most of these concern the desirability of increasing the bandwidth of the cooling system by raising the operating frequency range. However, before discussing these, let us review the situation for systems which are *not* power limited.

Based on Eq. 2, which applies to such non-power-limited systems, raising the frequency is clearly desirable, at least in principle. Let us assume for definiteness that we have a cooling system which operates over a one-octave frequency range, and we seek to double the bandwidth by doubling the mid-band frequency. If the system is mixing-limited, in addition to the factor of 2 improvement in  $W$ , an additional factor of two results from halving  $M$ .

A similar additional factor is usually obtained for noise-limited systems as well. Under the combined assumptions that the length of individual pickup elements is proportional to the operating frequency, that it is possible to preserve the same pickup impedance for the higher frequency electrodes, and that the total space available for electrodes remains unchanged, doubling the operating frequency permits a doubling of the number of electrodes, and hence a halving of  $U$  and a doubling of the cooling rate. In practice, this gain is partially offset by the increases in the preamplifier noise temperature and external circuit attenuation which accompany an increase in operating frequency. Hence overall, the cooling rate increases proportional to something between the first and second power of  $f_B$ .

Let us now turn our attention to the power-limited system. From Eq. 6b, we see that the quantity which best characterizes the performance of such a system is  $\tau_p$ , which is defined by Eq. 7a, and is most easily calculable using Eq. 10. For  $G_{lim}/G_{opt} \ll 1$ , the power-limited cooling rate  $\tau_{lim}^{-1}$  is simply given by  $2 \cdot \tau_p^{-1}$ ; as the gain ratio approaches unity (as for example, the beam cools), the rate falls by a factor of 2 to  $\tau_p^{-1}$ , while at the same time  $\tau_{opt}$  approaches  $\tau_p$ . As the ratio exceeds unity, the system is of course no longer power limited, and the maximum cooling rate is determined by  $\tau_{opt}$  from Eq. 2. The situation is illustrated in Fig. 1, where we have replaced  $\tau_{lim}$  by  $\tau_{opt}$  in the region where the gain ratio would exceed unity.

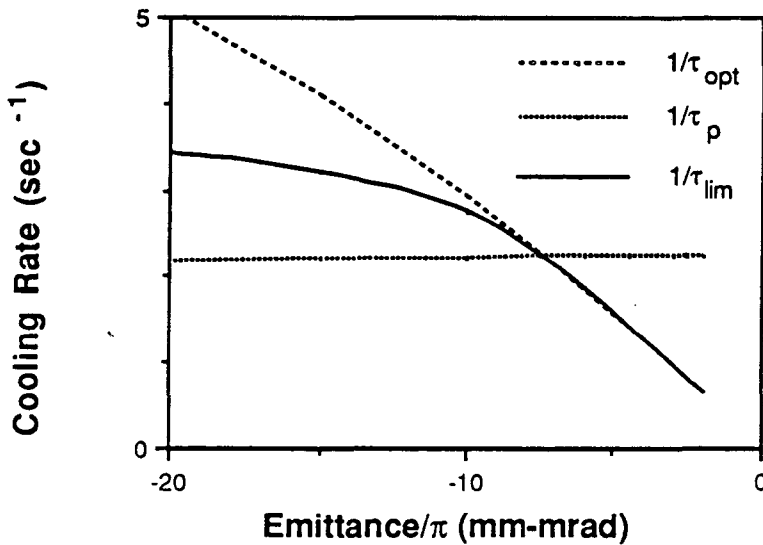


Fig. 1



Once one has calculated both  $\tau_p$  and  $\tau_{opt}$ , one can easily calculate  $G_{lim}/G_{opt}$  using Eq. 11a to obtain  $\tau_{lim}$  from Eq. 6b. One then integrates Eq. 16 numerically to determine the total cooling time from  $\epsilon_i$  to  $\epsilon_f$ . If, in the course of cooling, the emittance is reduced sufficiently that the system emerges from its power limited condition (see Fig.1), then, when integrating in Eq. 16, one uses the same procedure as used in graphing Fig.1, i.e. taking  $\tau(\epsilon)$  to be  $\tau_{lim}$  for  $G_{lim}/G_{opt} < 1$ , and to be  $\tau_{opt}$  for  $G_{lim}/G_{opt} > 1$ . The results of a set of such calculations are given in the following section for the Fermilab debuncher ring under a variety of cooling "scenarios;" however, before discussing them in detail, it is worthwhile to consider the systematic trends implied by the above equations.

Using  $\tau_p^{-1}$  as our figure of merit, we see from Eq. 10 that most, if not all, the advantage in going to higher frequency is lost when the system is power-limited. The doubling of  $n_A$  made possible by the reduced electrode length is offset by the factor of  $fB$  in the denominator, which arises from the  $1/f$  dependence of the kicker constant (this is based on the reasonable assumption that it is the transfer impedance, rather than the kicker constant, which one can preserve when raising the frequency). Also, because  $G_{lim}$  decreases as  $W^{-1/2}$  due to the increased noise bandwidth at higher frequency, the explicit  $W$ -dependence of  $\tau_p^{-1}$  is as the one-half power, rather than the usual linear one. Moreover, this improvement is likely to be at least partly offset (possibly even *more than offset*) by increases in attenuation and amplifier noise which usually characterize a frequency increase.

To improve the performance of power-limited systems, then, in most cases one must either increase the available amplifier power, decrease the input noise power, increase the detector impedance, or increase the number of arrays, presumably by managing to increase the longitudinal density of the pickups (by means other than raising the frequency). The first two of these are being undertaken by Fermilab and the third is a goal which has been pursued for non-power-limited systems as well, more or less continually.<sup>1</sup> We have recently managed to achieve the fourth as the serendipitous outcome of an effort to design a higher frequency pickup [1]; as with the increase in impedance, this factor will improve the performance of *non*-power-limited (albeit noise-limited) systems as well. (It might seem that reduction of input noise would benefit such systems as well; however, some schemes for doing this, such as the use of notch filters to eliminate interband noise, benefit only power-limited systems.)

As noted above, it may be possible that the cooling of the beam causes the system's operating range to span both the power-limited and noise-limited regimes; this, as we shall see, is the case for the debuncher in its proposed upgrade mode. For such systems, the situation is a bit more complicated. At first glance, it might seem that for such a system, doubling the operating frequency, which as we have noted will yield little or no improvement in  $\tau_p$ , will leave the cooling rate unaffected, at least in the power-limited portion of the cycle. However, because of the additional factor of  $2 \cdot G_{lim}/G_{opt}$  in the expression for  $\tau_{lim}$  (Eq. 6b), an improvement is in fact realized.

The situation is seen most easily by referring to Fig. 1. Because doubling the frequency results in increasing  $\tau_{opt}^{-1}$  by something like a factor of four, the curve for  $\tau_{opt}^{-1}$  for the higher frequency system would lie above the one shown and, *even assuming no improvement in  $\tau_p$* , its intersection with the  $\tau_{opt}^{-1}$  would occur at a lower (less than half as great) emittance. Therefore not only would the value of  $\tau_{lim}^{-1}$  be larger (i.e., more nearly equal to  $2 \tau_p^{-1}$ ) initially, but it would remain larger out to smaller values of emittance. (Beyond the intersection point, of course, the cooling rate would be improved by the full factor of  $\approx 4$ .) Hence, such a system can benefit from a doubling of the operating frequency, albeit by less than would a completely non-power-limited one.

---

<sup>1</sup>Moving the electrodes to follow the decreasing beam size is an example in this category.

We should note that there is actually a *fifth* approach for improving the performance of systems which are power-limited over their entire operating range. It is often possible to increase the impedance of a detector, at the expense of either increased length or reduced bandwidth, i.e. under the constraint that  $Z^2W/\ell \sim Z^2Wn_L$  remain constant. (CERN has, for other reasons, done something similar by making series-pairs out of its stripline loops, thereby roughly doubling both impedance and length, and halving bandwidth.) Since this product is also the figure of merit for a noise-limited cooling system, increasing  $Z$  in this manner does not improve the performance of such a system. On the other hand, for a power-limited system, in which the cooling rate increases only as the *square root* of the bandwidth, increasing the detector impedance in this fashion would result in a net performance gain.

Finally, we note the following subtle difference for a power limited system—the scaling of cooling time with beam emittance. Suppose that one wished to accommodate a beam of larger initial emittance by increasing the electrode gap as  $\sqrt{\epsilon}$ . Since  $Z_L'$  decreases as the reciprocal of the gap, Eq. 12 shows that for the two geometries,  $U$  would be the same when the beam had the same *fraction* of its initial emittance. Hence from Eq. 1 we see that for the *non*-power-limited system, the total cooling time to a given fraction of the initial emittance is unaffected by the scaling.

On the other hand, for power-limited systems, the scaled system comes off worse in two regards: Firstly, during the power-limited part of the cooling cycle, the cooling rate is lower; secondly, the point at which the system emerges from being power-limited depends on the *absolute* emittance, and *not* on the *fraction* of the initial emittance. The former result can be deduced from Eq. 10, where we see that  $\tau_p$  depends only on  $Z_L'$ , and not on the beam emittance. To deduce the latter result, note that emergence from the power-limited condition occurs at the point that  $G_{lim}/G_{opt} = 1$ . In the limit that  $U \gg M$ , Eq. 14 shows that this point depends only on the emittance, and not on  $Z_L'$ ; in fact if one examines the more general expression, Eq. 11b, one sees that to second order, the emittance at which  $G_{lim}/G_{opt} = 1$  *decreases* slightly as  $Z_L'$  becomes smaller. The latter result implies that for the system with the larger emittance, a lower cooling rate will be experienced over a larger portion of the cooling cycle; therefore the total time required to reach the same *fraction* of the initial impedance will be greater.

### Application to the Debuncher Upgrade

We now consider how the above results apply to the proposed upgrade of the Fermilab debuncher ring. The present debuncher is required to cool a beam of  $10^7$  particles from an rms emittance of  $20\pi/3$  to  $7\pi/3$ , in a cycling time of two seconds. The goal for the long-term improvement is to be able to cool a beam of  $4 \times 10^7$  particles from  $20\pi/3$  to  $2\pi/3^2$  in a cycling time of .75 sec.

Two improvements in the existing electronics are currently being undertaken to ameliorate the severely power-limited condition of the present system. By themselves, they will not suffice to meet the above goals. The first is a straightforward increase in the maximum power available by doubling the number of output TWT's in the transverse cooling system. The second the introduction of a notch filter in the low-level electronics to suppress the noise signal *in between* the betatron sidebands. The effect of this filter is ideally to reduce the noise bandwidth in the expression for  $G_{lim}$  by a factor of 2; note that because it suppresses the noise only at frequencies at which the noise does *not* heat the beam, this change leaves the value of  $U$  unaffected (however, the signal power term in Eq. 9 must now be changed from  $1/U$  to  $2/U$ ). In considering the effect of these upgrades on the present system, we have assumed that the available output power increases by somewhat more than a factor of two, from 1 kW per plane to 2.5; it is anticipated that with fewer splitters in the output circuit there will be less reflected power, and so the output tubes

<sup>2</sup>An alternate specification is  $30\pi/3$  to  $3\pi/3$ ; the ramifications of this alternative are discussed below.

can be run closer to their maximum output rating of 200W (a total output power of 3.2 kW). We have also assumed ideal notch filter performance, i.e. no degradation of the signal and a noise bandwidth reduction of the full factor of 2.

We consider four basic cooling systems: a 2-4 GHz system using the present set of electrodes but with upgraded electronics referred to above, a similarly upgraded 2-4 GHz system using the new type of bi-planar<sup>3</sup> detector [2] (effectively twice the number of detectors in the present system), a 4-8 GHz system employing more or less conventional striplines (again, twice the number of detectors in the present system) which, to distinguish it from the bi-planar system, we will refer to as "uni-planar"<sup>4</sup>, and a 4-8 GHz system with a bi-planar detector (and hence four times the number of detectors in the present system).<sup>5</sup>

For reasons which will become apparent, we consider both 4-8 GHz systems at maximum power levels of 2.5 kW (the same output power capability as the 2-4 GHz system) and 5 kW; despite the anticipated difficulty in producing a noise-reduction filter for 4-8 GHz, we have included the effect of such a filter for the 4-8 GHz system as well. We consider each system at intensities of  $N=1, 4$ , and  $8 \times 10^7$ ; even though this last level exceeds the maximum presently conceived intensity, we felt it prudent to examine it so as to ensure that the choice of cooling system would not preclude utilizing such an intensity increase. The remaining system parameters used in our calculations are listed in Table 1. In addition, a list of the assumptions made in the calculations (some of which have already been stated in the text) is presented in Appendix I.

A summary of the results of the calculations is presented in Table 2, where the cooling times from an initial (full) emittance of  $20\pi$  to emittances of  $7\pi$ ,  $4\pi$ , and  $2\pi$  are tabulated for each of the cooling scenarios. Along with the times, the corresponding values of  $G_{lim}/G_{opt}$  are presented to show the points at which the cooling system ceases to be power-limited. More detailed results, showing all of the calculated quantities at a number of intermediate emittances, as well as the results for an initial (full) emittance of  $30\pi$ , are presented in Appendix II.

Several observations are worth noting. Firstly, the 2-4 GHz systems cease to be power-limited at emittances below  $7\pi$ ; hence little further improvement can be effected by further increasing their power capabilities. In contrast, the 2.5 kW 4-8 GHz systems remain power-limited down to nearly the smallest emittance; hence we felt it reasonable to calculate the effect on their performance of an additional doubling of the output power to 5 kW.

As anticipated, the bi-planar 4-8 GHz system outperforms the parallel plate system by roughly a factor of two throughout, by virtue of having twice as many electrodes (which, as noted above, doubles its performance in both the power-limited and non-power limited regimes). What is perhaps more surprising, is that even for the highest planned intensity (i.e.  $N = 4 \times 10^7$ ), this advantage enables the 2-4 GHz bi-planar system to yield cooling times comparable to those obtained with a 4-8 GHz parallel plate system having the same total output power<sup>6</sup>. In fact, in the

<sup>3</sup>i.e., a detector capable of sensing motion in both transverse planes simultaneously.

<sup>4</sup>Fermilab has recently developed a design for a 4-8 GHz detector [3], employing striplines arranged in two parallel arrays in order to achieve adequate lateral coverage of the beam, which they feel can also be used as a bi-planar detector, although its performance appears inferior to the corner detector of Ref. 1. We have adopted the "uni-planar"/"bi-planar" designations as a way of avoiding the separate issue of which design makes for a superior bi-planar detector.

<sup>5</sup>Our initial models of the bi-planar corner detector appear to show that the longitudinal loop separation can be reduced to the point that the longitudinal loop density can be increased by possibly as much as 40%; however to keep our estimates conservative, we have neglected this factor in our calculations.

<sup>6</sup>The comparison is most favorable to the uni-planar system for the smallest final emittance; at this point the system is no longer power-limited, and is therefore able to realize the full advantage of the higher operating frequency. Such small emittances are generally achieved only relatively late in the cooling cycle.

Table 1. Assumed Parameters for Various Choices of Electrodes

System Parameter	Upgraded 2-4 GHz	Bi-Planar 2-4 GHz	Uni-Planar 4-8 GHz	Bi-Planar 4-8 GHz
$f_B$ (GHz)	3	3	6	6
W (GHz)	2	2	4	4
$T_R + T_A$ ( $^{\circ}$ K)	140	140	180	180
$\alpha, \alpha_p$	0.64	0.64	0.5	0.5
M	10	10	5	5
$G_{im}^* (V_{out}/V_{in})$	$3.59 \times 10^7$	$3.59 \times 10^7$	$1.59 \times 10^7$	$1.59 \times 10^7$
(dB)	151	151	147	147
$n_L$	128	256	256	512

\*Gain figures for 4-8 GHz are for  $P_{out} = 2.5$  kW (per plane); for 5 kW system values are 3 dB greater

Common parameters:

$$Z_L' = 20 \Omega/cm$$

$$Z_c = 50 \Omega$$

$$\beta = 10 m$$

$$E/e = 8.938 GV \text{ (K.E. = 8 GeV)}$$

$$f_o = .590 MHz$$

absence of notch filters at the higher frequency, the 2-4 GHz bi-planar system would outperform the 4-8 GHz uni-planar system!

There are two disappointing notes. The first is that even assuming the availability of a 4-8 GHz notch filter, the bi-planar 4-8 GHz system will require a doubling of the (already upgraded) output power to 5 kW in order to achieve the desired emittance cooling within the required (.75 sec) time. The second is that were one to increase the debuncher acceptance to  $30\pi$ , as is being considered at present, the final emittance achieved after the same total cooling time (assuming the detector can be scaled) would be  $4\pi$ , consistent with the failure of power-limited systems to scale, as noted earlier. It is true that the calculation was somewhat conservative in neglecting the increased longitudinal packing density which this design appears to permit. On the other hand, this may be offset by in the fact that possible adverse effects from non-linear response and the larger betatron phase advance spanned by these arrays have been neglected.

### Acknowledgements

In writing this paper, we have benefitted from discussions with the  $\bar{p}$ -source group at Fermilab. We are particularly indebted to John Marriner (who originally brought this problem to our attention) for his ready availability to answer questions about the operation of the Fermilab  $\bar{p}$  source and his careful reading of the draft version of this manuscript.

Table 2: Calculated Debuncher Performance

N	$\frac{\epsilon}{\text{---}}$	Upgraded 2-4 GHz System (2.5 kW)		Bi-Planar 2-4 GHz System (2.5 kW)		Uni-Planar 4-8 GHz System (2.5 kW)		Bi-Planar 4-8 GHz System (2.5 kW)		Uni-Planar 4-8 GHz System (5 kW)		Bi-Planar 4-8 GHz System (5 kW)	
		$\frac{G_{lim}}{G_{opt}}$	$T_{tot}$ (sec)	$\frac{G_{lim}}{G_{opt}}$	$T_{tot}$ (sec)	$\frac{G_{lim}}{G_{opt}}$	$T_{tot}$ (sec)	$\frac{G_{lim}}{G_{opt}}$	$T_{tot}$ (sec)	$\frac{G_{lim}}{G_{opt}}$	$T_{tot}$ (sec)	$\frac{G_{lim}}{G_{opt}}$	$T_{tot}$ (sec)
$1 \times 10^7$	$20\pi/3$	.38	—	.43	—	.14	—	.15	—	.20	—	.16	—
	$7\pi/3$	.99	.74	1.0	.39	.39	.57	.40	.29	.55	.43	.56	.22
	$4\pi/3$	1.7	1.4	1.7	.74	.67	.93	.68	.47	.94	.73	.96	.37
	$2\pi/3$	3.3	3.0	3.4	1.5	1.3	1.6	1.3	.79	1.9	1.4	1.9	.69
$4 \times 10^7$	$20\pi/3$	.52	—	.69	—	.17	—	.21	—	.24	—	.29	—
	$7\pi/3$	1.1	.85	1.3	.51	.42	.60	.46	.32	.59	.46	.65	.25
	$4\pi/3$	1.8	1.6	2.0	.95	.70	.97	.74	.52	.99	.77	1.1	.42
	$2\pi/3$	3.5	3.3	3.7	1.9	1.4	1.6	1.4	.86	1.9	1.4	2.0	.76
$8 \times 10^7$	$20\pi/3$	.69	—	.98	—	.21	—	.27	—	.29	—	.38	—
	$7\pi/3$	1.3	1.0	1.7	.72	.46	.64	.53	.36	.65	.50	.76	.29
	$4\pi/3$	2.0	1.9	2.4	1.3	.74	1.0	.82	.58	1.1	.83	1.2	.48
	$2\pi/3$	3.7	3.7	4.1	2.3	1.4	1.7	1.5	.96	2.0	1.5	2.1	.86

↓

References

1. "Physics and Technique of Stochastic Cooling," D. Möhl, G. Petrucci, L. Thorndahl, and S. van der Meer, CERN/PS/AA 79-23, 1979 (unpublished).
2. "Novel Electrode Design for a 4-8 GHz Stochastic Cooling System," D.A. Goldberg, J.K. Johnson, G.R. Lambertson, and F. Voelker, Bull. Am. Phys. Soc. **33**, 1025, (1988).
3. "4-8 GHz Pickup Design for the pbar Accumulator," S.Y. Hsueh, Bull. Am. Phys. Soc. **33**, 1025, (1988).

APPENDIX I

Below are listed the characteristics of the cooling systems that have been assumed in the calculation of cooling times.

2.5 kW output power is attainable when the number of TWT's is doubled.

An ideal notch filter (factor of two reduction in noise bandwidth; no signal loss) is available at both 2-4 GHz and 4-8 GHz.

Electrodes are not plunged.

Effects of non-linearity in (position) response are ignored.

For the bi-planar arrays, the following additional assumptions are made:

No performance reduction due to combining signals over 60° of betatron phase advance.

Increased longitudinal density of biplanar electrode structure relative to existing electrodes is ignored

The aspect ratio of bi-planar arrays can be changed without affecting their sensitivity.

Signals from bi-planar arrays having different aspect ratios can be combined without penalty.

A 20  $\Omega$ /cm-perr-module transfer impedance in both planes is assumed.

APPENDIX II: DETAILS OF COOLING TIME CALCULATIONS

For convenience in calculating, we can rewrite Eqs. 4, 9, 10, 11b, 12, and 14 with the various physical constants lumped together in a single constant, whose value is then suitably modified so that the remaining quantities can all be expressed in "conventional" units, as shown below.

$$G = \frac{1.081 \times 10^{-12} f_o(\text{MHz}) \bar{\beta}(\text{m}) \alpha N(10^7) n_L [Z'_L(\Omega/\text{cm})]^2}{E/e(\text{GV}) f_B(\text{GHz}) Z_c(\Omega)} \quad (4')$$

$$G_{\text{lim}} = 2.692 \times 10^8 \sqrt{\frac{P_{\text{out}}(\text{kW})}{(1 + \frac{1}{U})(T_R + T_A) W(\text{GHz})}} \quad (9')$$

$$\frac{1}{\tau_p}(\text{sec}^{-1}) = \frac{2.910 \times 10^{-2} f_o(\text{MHz}) \bar{\beta}(\text{m}) \alpha n_L [Z'_L(\Omega/\text{cm})]^2}{E/e(\text{GV}) f_B(\text{GHz}) Z_c(\Omega)} \sqrt{\frac{P_{\text{out}}(\text{kW}) W(\text{GHz})}{(1 + \frac{1}{U})(T_R + T_A)}} \quad (10')$$

$$\frac{G_{\text{lim}}}{G_{\text{opt}}} = \frac{2.910 \times 10^{-4} f_o(\text{MHz}) \bar{\beta}(\text{m}) \alpha n_L [Z'_L(\Omega/\text{cm})]^2 N(10^7) (M+U)}{E/e(\text{GV}) f_B(\text{GHz}) Z_c(\Omega)} \cdot \sqrt{\frac{P_{\text{out}}(\text{kW})}{(1 + \frac{1}{U})(T_R + T_A) W(\text{GHz})}} \quad (11b'')$$

$$U = \frac{3.379 \times 10^4 (T_R + T_A) Z_c(\Omega)}{N(10^7) f_o(\text{MHz}) \beta_x(\text{m}) \bar{\epsilon}(\text{mm}\cdot\text{mrad}) \alpha_p^2 n_L [Z'_L(\Omega/\text{cm})]^2} \quad (12')$$

$$\frac{G_{\text{lim}}}{G_{\text{opt}}} = \frac{9.831}{E/e(\text{GV}) f_B(\text{GHz}) \bar{\epsilon}(\text{mm}\cdot\text{mrad})} \frac{\bar{\beta}}{\beta_x} \frac{\alpha}{\alpha_p^2} \sqrt{\frac{P_{\text{out}}(\text{kW})(T_R + T_A)}{W(\text{GHz})}} \quad (14')$$



In particular, for the case of the TeV-I debuncher, Eqs. 8, 10, and 12 (the formulas required to produce the tables in the present report) can be further simplified by substituting in the debuncher parameters of 8 GeV kinetic energy, 590 kHz revolution frequency, and a mean beta function of 10 m, as well as a characteristic impedance of 50 ohms to yield the following equations:

$$G = \frac{1.825 \times 10^{-12} \alpha n_A [Z'_L (\Omega/cm)]^2 N (10^7)}{f_B (\text{GHz})} \quad (8'')$$

$$\frac{1}{\tau_p} (\text{sec}^{-1}) = \frac{4.917 \times 10^{-2} \alpha n_A [Z'_L (\Omega/cm)]^2}{f_B (\text{GHz})} \sqrt{\frac{P_{\text{out}} (\text{kW}) W (\text{GHz})}{(1 + \frac{1}{U}) (T_R + T_A)}} \quad (10'')$$

$$U = \frac{2.237 \times 10^3 (T_R + T_A)}{\alpha_p^2 N (10^7) n_A \bar{E} (\text{mm} \cdot \text{mrad}) [Z'_L (\Omega/cm)]^2} \quad (12'')$$

where, to further simplify matters, we have used  $n_A$  to denote the number of 128-loop arrays.

The tables on the following pages present the detailed results of the cooling calculations for the six scenarios described in the main text. Tables 1 and 2 are for an initial r.m.s. emittance of  $20\pi/3$ ; Tables 3 and 4, of  $30\pi/3$ . Eqs. 12'' and 10'' were used to calculate  $U$  and  $\tau_p^{-1}$ , respectively;  $\tau_{\text{opt}}$  was calculated using Eq. 2, and  $G_{\text{lim}}/G_{\text{opt}}$  was then obtained using Eq. 11a. For  $G_{\text{lim}}/G_{\text{opt}} < 1$ , the numbers in the column labelled  $\tau_{\text{lim}}$  represent the results calculated using Eq. 6b; for  $G_{\text{lim}}/G_{\text{opt}} > 1$ , they are simply  $\tau_{\text{opt}}$ .  $T_{\text{tot}}$  was calculated from Eq. 16 using trapezoidal integration. Finally the notes for the two 2-4 GHz calculations show how the above equations were modified to take into account the effects of the noise-suppressing notch filter.

*LAWRENCE BERKELEY LABORATORY  
TECHNICAL INFORMATION DEPARTMENT  
UNIVERSITY OF CALIFORNIA  
BERKELEY, CALIFORNIA 94720*